PCCP

Accepted Manuscript

ROYAL SOCIETY OF CHEMISTRY

www.rsc.org/pccp

Journal Name

RSCPublishing

ARTICLE

Cite this: DOI: 10.1039/x0xx00000x

Received 00th January 2012,
Accepted 00th January 2012

DOI: 10.1039/x0xx00000x

www.rsc.org/

Water-wetting surfaces as hydrate promoters during transport of carbon dioxide with impurities

Tatiana Kuznetsova, Bjørnar Jensen, Bjørn Kvamme[a], Sara Sjøblom

Water condensing as liquid drops within the fluid bulk has traditionally been the only scenario accepted in the industrial analysis of hydrate risks. We have applied a combination of absolute thermodynamics and molecular dynamics modeling to analyze the five primary routes of hydrate formation in a rusty pipeline carrying dense carbon dioxide with methane, hydrogen sulfide, argon, and nitrogen as additional impurities. We have revised the risk analysis of all possible routes in accordance with the combination of the first and the second laws of thermodynamics to determine the highest permissible content of water. It was found that at concentrations lower than five percent, hydrogen sulfide will only support formation of carbon dioxide-dominated hydrate from adsorbed water and hydrate formers from carbon dioxide phase rather than formation in the aqueous phase. Our results indicate that hydrogen sulfide leaving the carbon dioxide for the aqueous phase will be able to create an additional hydrate phase in the aqueous region adjacent to the first adsorbed water layer. The growth of hydrate from different phases will decrease the induction time by substantially reducing the kinetically limiting mass transport across the hydrate films. Hydrate formation via adsorption of water on rusty walls will play the decisive role in hydrate formation risk, with the initial concentration of hydrogen sulfide being the critical factor. We concluded that the safest way to eliminate hydrate risks is to ensure that the water content of carbon dioxide is low enough to prevent water dropout via adsorption mechanism.

[a] *Universitetet i Bergen, Institutt for Fysikk og Teknologi, Allégaten 55, N-5007 Bergen, Norge. Fax: +47 55589440; Tel: +47 55583310; E-mail: bjorn.kvamme@ift.uib.no*

Introduction

Pipeline transport of large volumes of carbon dioxide at low temperatures and high pressures has recently become a topic of high interest due to the growing number of sequestration projects that require moving large volumes carbon dioxide underground storage destinations. Carbon dioxide to be transported is either produced together with hydrocarbons, from gas fields in the North Sea and carbon dioxide-rich offshore gas reservoirs in Malaysia and Indonesia, or separated from the flue gas. Carbon dioxide is well known to aggressively form crystalline ice-like compounds, called clathrate hydrates [1 and references therein]. When allowed to grow unchecked, the hydrate formation can severely obstruct the flow, resulting in blockage of pipeline and potential damage to equipment. Despite the rusty pipeline walls offering excellent sites for adsorption of water [2] and thus adding additional pathways for hydrate formation, traditional industrial analysis of hydrate risk has been based on dew-point calculations. In the case of increasingly relevant seafloor transport of carbon dioxide, the wall will normally be at low, quite possibly near-zero, temperature. One should also keep in mind that heterogeneous nucleation and growth on solid surfaces is kinetically favored in comparison with crystallization from bulk. The transport of carbon dioxide with impurities is the main focus of this study, and we will limit ourselves to water, hydrogen sulfide, methane, nitrogen, and argon as said impurities.

Carbon-dioxide-transporting pipelines on the seafloor will be typically exposed to temperatures ranging from 1 to 6 degrees Celsius and pressures of 50 to 250 bars. This would mean that three of the above-mentioned impurities (argon, hydrogen sulfide and nitrogen) will be supercritical and soluble in carbon dioxide. This fact will have a certain impact in hydrate formation since the impurities can both enter the hydrate structure as cavity-filling “guests” and modify the properties of carbon dioxide. Hydrogen sulfide, on the other hand, has a critical point at 373 K and 89 bars and is soluble as an acid in water. As a result, its impact on the routes to hydrate formation will be substantially different from that of other impurities. Condensation of water from carbon dioxide is likely to be accompanied by that of hydrogen sulfide, which will in turn affect the hydrate formation. Similar factors will be in play in case of adsorption on water-wetting surfaces like hematite (Fe_2O_3), the dominant rust form. Although hydrogen sulfide has a lower dipole moment than water, its molecular geometry and charge distribution are similar, thus once can expect similarities in adsorption characteristics.

The Gibbs phase rule expresses the conservation of mass under the constraints of thermodynamic equilibrium. In case of four phases (fluid, water, adsorbed, hydrate) and two components (carbon dioxide and water), given that temperature and pressure will be locally defined, the phase rule will results in zero degrees of freedom and the system will be overdetermined. One could argue that adding two more components to the fluid phase without changing the number of possible phases would change the situation and theoretically allow the system to reach equilibrium. The combined first and second laws of thermodynamics will, however, direct the system to all the states with the lowest free energy possible at the given point. The initial hydrate formation will be governed by the presence of hydrogen sulfide, an excellent hydrate former due to electrostatic attraction between hydrogen sulphide’s hydrogen and cavity water oxygen [3]. This will lead to the most stable hydrates forming first due to the very high driving forces.

Hydrate formation is generally the consequence of the lowered entropy of water brought about by presence of hydrate former – and the subsequent reorganization of water molecules to optimize the entropy change. Phase transition kinetics will be ultimately governed not just by the intrinsic phase transition kinetics but also the associated kinetics of mass and heat transport. During a heterogeneous hydrate formation at the interface between water and gas phases, hydrate formers must be transported to the water, adsorbed on the interface and incorporated into hydrate structures on the gas side of the

interface or they can dissolve into the liquid side of the interface and rearrange it into hydrate-like structures. In either case, both hydrogen sulphide [4] and carbon dioxide [5, 6] will vigorously adsorb on the gas side of the liquid water interface. As shown in [3], the average orientation of water incorporated into the hydrate lattice will impose a certain electrostatic potential field inside the hydrate cavity. This potential will be significantly negative at those locations where the outer CO2 atoms (oxygen) are most likely to reside, irrespective of the particular force-field chosen, resulting in net electrostatic repulsion between carbon dioxide and water in addition to attractive van der Waals interaction.

Yet another difference between carbon dioxide and hydrogen sulphide lies in the size of their molecules. In order to isolate the electrostatic impact, a non-polar spherical model for carbon dioxide was investigated by Kvamme & Tanaka [1]. It was found that the intra-cavity motion of carbon dioxide appeared to interfere with several librational frequencies of the TIP4P water molecules in hydrate lattice, resulting in a roughly 1 kJ/mol penalty at 0 Celsius. No similar penalties were observed in the case of hydrogen sulphide, indicating that H_2S did not appear to disturb the hydrate lattice, a fact also reflected in substantially different hydrate equilibrium curves. Given that dynamic steps involved in hydrate formation from either hydrogen sulphide or carbon dioxide are fundamentally similar, it is the availability of hydrate formers and free energy gain that determines which hydrate will form first. The formation process will involve a gradually changing hydrate composition and correspondingly varying free energy of the system. As discussed in our earlier papers [2, 6 -- 10], hydrate of different compositions and densities will constitute thermodynamically separate phases, further complicating the application of the Gibbs phase rule. While a more stable hydrate will never reform into a less stable hydrate, a less stable hydrate will require access to new hydrate formers to be able to reform into a more stable hydrate. The latter option will be a possibility under continuous flow. In addition, hydrate may also dissolve when in contact with under-saturated phases and reform. From a dynamic point of view, it is however unlikely that any state of hydrate equilibrium can be reached during the pipeline flow of carbon dioxide with impurities.

Figure 1 below summarizes routes relevant for hydrate formation and possible re-dissociation on the basis of the Gibbs free energy change associated with their phase transitions, ΔG_i:

$$\Delta G_i = \delta \left[x_w^{H,i}\left(\mu_w^{H,i} - \mu_w^{\rho}\right) + \sum_{j=1}^{n_H} x_j^{H,i}\left(\mu_j^{H,i} - \mu_j^{p}\right) \right] \quad (1)$$

Equation (1) utilizes the standard expression for the Gibbs free energy per mole, $G = \Sigma x_k \mu_k$, based on the fact that G is a function of two intensive (T, P) and one extensive variable. In the equation, x is the mole fraction, μ is chemical potential, k runs over all components; 'H' denotes the hydrate phase, 'i' represents any of the six phase transition scenarios outlined in Figure 1, 'p' stands for any of the liquid, gas and adsorbed phases, subscript j indicates any hydrate guest species and runs over all hydrate formers n_H participating in route i. Factor δ will be 1 for hydrate formation or reformation and -1 in case of hydrate dissociation. Given that phases are not in equilibrium, hydrates created along the different pathways will have different filling fractions and free energies, with each hydrate-forming process thus resulting in a unique phase.

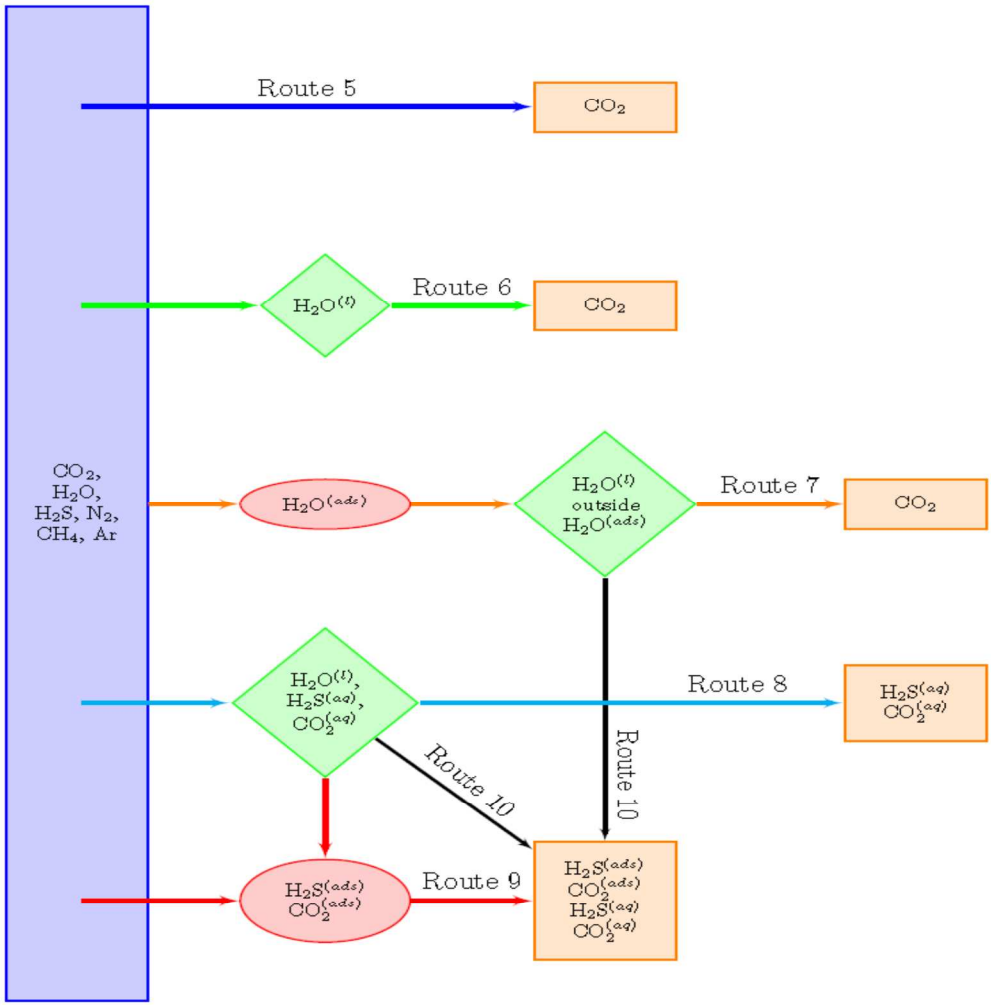

Figure 1. Schematic illustration of routes relevant for hydrate formation from water and impurities entrained in dense CO_2 phase. Text inside the coloured boxes lists guest species involved in hydrate formation, with superscript indicating the phases they originate from. The brown boxes correspond to the formed hydrate phases, green diamonds are aqueous phases, red ellipses are phases adsorbed on hematite. For continuity's sake, we keep the enumeration scheme used in our previous work [2, 10] and thus start at Route 5.

The negativity of ΔG_i in equation (1) is the absolute minimum requirement for the phase transition i to be possible according to the first and the second laws of thermodynamics. According to the modern nucleation theory, this difference has to be large enough to overcome penalty associated with creating space for the new phase. In case of homogeneous hydrate formation from liquid water, this work will be proportional to the interface free energy and the contact area between hydrate and surrounding liquid water. When hydrate forms on the interface between liquid water and the hydrate former phase, the picture can become even more complicated, for example, the hydrate core facing the hydrate formers might also be partially wetted due to capillary forces. In case of equilibrium or quasi-equilibrium calculations, these nanoscale details are of little import. What matters more is that equation (1) and associated penalty terms are the thermodynamic contributions to phase transition kinetics, with kinetics of associated mass- and heat-transport being the two other contributions. So regardless of how negative the ΔG_i in equation (1) may be, the phase transition will not proceed without a supply of mass and adequate heat transport to move away the released heat. This might actually prevent Route 5 from presenting any realistic risks [2].

Codes currently available for industrial hydrate risk evaluation restrict their analysis to route 6 via pressure and temperature projections of the phase stability boundaries. In practice, they implement a

simple two-step routine which first determines the likelihood of water condensing in the fluid phase and subsequently evaluates the hydrate equilibrium in terms of pressure and temperature alone for the given gas/fluid composition. Few (if any) open commercial and academic codes are capable of evaluating homogeneous hydrate formation from solution of hydrate formers dissolved in water. There are no available hydrate codes that can evaluate heterogeneous hydrate formation under influence of solid surfaces, despite numerous pictures and examples of hydrate films dominated by growth on solid surfaces, even in absence of flow. A more rigorous approach would be to develop a scheme for free energy minimization which would also incorporate mass transport and heat transport as its minimum constraints. Strictly speaking, hydrodynamic effects will also need to be included in cases where rapid dissociation can result in formation of separate fluid phases upon the release of hydrate formers.

The challenge of considering both non-equilibrium thermodynamics and competing hydrate phase transitions can be handled on different levels. Strategies discussed elsewhere (see [2, 9] and references therein) have been supplemented in this paper by corresponding equations for the cases of sub- and super-saturation. Analysis based on equation (1) and scenarios in Figure 1 can easily be simplified at the cost of some rigor, but would require some logistics and extensions of typical industrial hydrate codes. For a conservative analysis, one may skip the possible dissociation scenarios which would of course reduce the hydrate risk and focus on the possible routes to hydrate formation.

Route 5 has been investigated in [2] for a mixture of carbon dioxide and water and found to be thermodynamically feasible (though while disregarding any mass transport limitations, likely to be considerable in this case). Argon, nitrogen and methane at mole fractions below 0.05 are not likely to alter these conclusions substantially. The situation will be very different in case of hydrogen sulfide. Even at relatively low concentrations [11, 12], the presence of H_2S will increase the hydrate stability and result in formation of hydrates with different composition and free energies, as discussed above. But with the water mole fraction in CO_2 not rising above 10^{-3}, it would be questionable whether this route could play a significant role compared to the others. Surface reformation (Route 7) has been investigated both experimentally and theoretically, see examples elsewhere [7-9]. The stability regions of carbon dioxide hydrates in Kvamme [8, 10] will be shifted in the presence of water-soluble hydrogen sulfide but not significantly affected by argon, nitrogen and methane since the process involves homogeneous hydrate formation from aqueous solution. Adsorption of water on hematite has been investigated in [10], where it was shown that water may thermodynamic benefit substantial by adsorbing on hematite instead of condensing out as liquid water. This indicates that hydrate formation via routes 9 and 10 have a clear potential to outcompete routes 6 and 8.

This general scheme can easily be implemented as an extension of industrial hydrate risk evaluation codes in a possible events scheme, and corresponding levels of acceptable carbon dioxide content. Rigorous schemes like those developed in [2, 10] require consistent reference values for thermodynamics of all phases interacting with hydrate. Providing routes to absolute (with ideal gas as reference state) thermodynamic properties for all co-existing phases is also an important aspect of this paper. Models may be refined and extended but the approach presented here will provide a convenient starting point.

Atomistic simulations relevant for hydrate formation from adsorbed phases: potential pitfalls and possible solutions

Force fields developed to model crystals are normally fitted to reproduce certain measurable properties of the specific bulk crystal solids. In case of crystals containing ions, it is the partial charges that will dominate compared to the short-range repulsion and attractive forces. On the other hand, models used for water and fluid components like dissolved H_2S and CO_2 would have been typically matched to experimental data for bulk properties, with the cross terms sometimes corrected for better solubility and/or other mixture-relevant properties. The ranges of translational

and vibrational velocities in a liquid are quite different from those characteristic for the solid state, while the adsorbed phase may lie somewhere in between. Short-range interactions that can be safely ignored in the liquid-state models may have a substantially different impact for the adsorbed state. An example can be provided by the van der Waals term for the hydrogen, which is zeroed in widely accepted water force fields like SPC/E [13] and TIP4P [14]. As the result, the short-range potential on oxygen will implicitly include the influence of the "smeared out" hydrogen. Even for water models that explicitly include the Lennard-Jones contribution of the hydrogen, like for instance F3C [15], there is no guarantee that this short-range potential will be appropriate for description of the adsorbed state. There is no theoretical verification either that the van der Waals oxygen parameters in these models will be adequate in case of water adsorbed onto a mineral surface where the split between electrostatic and van der Waals forces has been decide from the best fit of bulk crystal properties.
These limitations of simplified water models make it tempting to assign separate and independent set of short-range cross term interactions between mineral and water. The existing integral equation theories ([16, 17]) offer fairly rigorous techniques that allow to quantify errors inherent in 'mixing and matching' cross terms based on combination rules for pure fluid substances and those specifically derived to describe fluid-mineral interactions.

An alternative to the independent assignment of short range atom-atom interactions can be provided by the use of mixing rules. In case of the Lennard-Jones potential, the Lorentz-Berthelot mixing rules will be given by:

$$\epsilon_{\alpha_M\gamma_K} = \sqrt{\epsilon_{\alpha_M\alpha_M}\epsilon_{\gamma_K\gamma_K}}\left(1 - k_{\alpha_M\gamma_K}\right) \quad (2)$$

$$\sigma_{\alpha_M\gamma_K} = \frac{1}{2}\left(\sigma_{\alpha_M\alpha_M} + \sigma_{\gamma_K\gamma_K}\right) \quad (3)$$

here $\varepsilon_{\alpha_M\gamma_K}$ is the Lennard-Jones well-depth of the cross interaction and $\sigma_{\alpha_M\gamma_K}$ is the Lennard-Jones diameter for the cross interaction. Equation (2) with $k_{\alpha_M\gamma_K}$ set to zero is historically based on observations of liquid mixtures near the critical point. As such, $k_{\alpha_M\gamma_K}$ can be considered an empirical parameter used to adjust the fit to match the relevant conditions rather than the critical density (roughly only 1/3 of liquid density). The use of mixing rules still would not solve the problem that the liquid state models may have when it comes to describing the adsorbed state, but it will preserve the consistency of description.

To match our earlier studies [10, 18 - 21] of pipeline transport of CO2, the impurities considered in this work have been limited to H2S and CH4. Methane, modelled using the united-atom OPLS Lennard-Jones model [22], has shown itself unable to compete with water for adsorption onto hematite surface [10, 18 - 20]. It should be noted thought that these findings did not preclude that CH4 could be trapped inside the density gaps of the water-dominated adsorbed layers [10, 20].

Thermodynamic analysis of phase transitions involved in hydrate formation in the presence of adsorbed phases

Our previous studies of water adsorption on hematite [6] indicate that chemical potential of water adsorbed on hematite may be lower than that of bulk water by as much as 3.4 kJ/mol. The hydrate formation on the surface of hematite will be therefore thermodynamically inhibited. But this adsorbed layer will extend only to about 3 – 4 water diameters, with water beyond this region

virtually non-affected by the solid surface and behaving similarly to bulk liquid water. The hematite surface will therefore serve as the primary water condensation site compared to homogeneous dropout of water inside the carbon dioxide phase. In addition, the hematite surface will also provide an adsorption surface for some of the hydrate formers. In a non-equilibrium system, hydrate will therefore be to form from water just over 1 nanometre away from the surface. Since the system will be unable to reach equilibrium as the consequence of the Gibbs Phase rule and/or combined the 1st and the 2nd laws of thermodynamics, the most appropriate way to analyse the system is by performing free energy minimization under constraints of mass and energy conservation. Under the relevant transport conditions, it is water concentration that will determine the dew-point as well as govern water condensation on the rusty surface. The first step of a simplified discrete analysis would therefore evaluate the maximum mole fraction of water that will be supported inside the carbon dioxide before dropping out as either liquid water, equation (4) or through adsorption on hematite, equation (5):

$$\mu_{w,liq}\left(T,P,\vec{x}_{liq}\right) \le \mu_{w,CO_2}^{id.gas}(T,P,\vec{y}) + RT\ ln\left[y_{w,CO_2}\phi_{w,CO_2}(T,P,\vec{y})\right] \quad (4)$$

$$\mu_{w,ads.}(T,P,\vec{x}_{ads.}) \le \mu_{w,CO_2}^{id.gas}(T,P,\vec{y}) + RT\ ln\left[y_{w,CO_2}\phi_{w,CO_2}(T,P,\vec{y})\right] \quad (5)$$

where subscript "w" denotes water. Subscripts "liquid" and "adsorbed" refer to liquid water phase and adsorbed phase, respectively. Similarly, subscript "CO2" stands for the CO2 phase. $\vec{x}$ is the mole fractions vector in the various phases as denoted by subscript, while $\vec{y}$ is the gas phase mole fractions. ϕ_{w,CO_2} is the fugacity coefficient for water dissolved in the CO2 phase.

The equality sign in equation (4) and (5) can only be valid if the system in question can reach equilibrium. But even for non-equilibrium systems, comparison of their respective equilibrium limits for $y_{w,CO2}$ would indicate which of the two routes will be thermodynamically favoured at given temperature and pressure.

When water drops out as adsorbed phase, the formation of hydrate can only happen beyond the immediate adsorbed layer. A further progress towards hydrate can continue both on the interface between water and carbon dioxide and from hydrate formers dissolved in water. These routes to hydrate formation have been discussed in more detail elsewhere [7, 8, 10, 18 – 21]. Most hydrate risk evaluation tools are based on liquid water formation through equation (5) and subsequent hydrate formation together with hydrate formers from the carbon dioxide phase. The adsorption of hydrate formers will present yet another route to hydrate formation from liquid water in parallel to these routes.

It was shown in Kvamme et.al. [10] that chemical potential of adsorbed TIP4P [14] water may be approximated by the following correlation resulting from interpolation between molecular dynamics simulations at 278 K and 245 K [7]:

$$\mu_{w,ads}(T) = \ [-56.2 - 0.1030(T - 278)] \quad kJ/mole \quad (6)$$

A minor pressure correction has been omitted in eq. (6). Any extrapolation beyond the fitted temperature range should be handled with caution. Since the main focus of this work is to illustrate the possible impact of the adsorbed phase on hydrate formation, it will suffice.

Molecular dynamics modelling of hematite-water-CO_2 system

Our hypotheses concerning the behaviour of carbon dioxide and water close to rusty surfaces were tested by performing molecular dynamic simulations of several model water-CO2-hematite systems at 274 K. Similar to our earlier studies of heterogeneous aqueous phases in contact with minerals [10, 20], the simulated system was constructed by stacking together two building blocks, a water layer and a slice of iron-terminated hematite crystal cleaved along its dominant [0001] surface. Two composite systems were created, both ranging 40.35 Å x 61.12 Å in x- and y-directions, while differing in the z-extension of the water phase (15 and 22 Å). They contained 1069 and 1655 water molecules, respectively, and 3 carbon dioxide molecules as the fluid phase, with the hematite crystal composed of 2016 iron atoms and 3024 oxygen molecules. The CO2 molecules were initially evenly distributed inside the bulk layer of the water phase, quite a distance away from the hematite surface.

The van der Waals interactions between water and hematite used the Buckingham-type potential with parameters from de Leeuw and Cooper [23], Tsuzuki *et al* [24] Buckingham type model with geometric combination rules was utilized for interactions involving CO_2 and hematite. The extended simple point charge (SPC/E) model of [13] was used to model water-water interactions. The water – CO_2 interactions were described by potential due to Panhuis *et al* [25], particularly successful in reproducing the behaviour of carbon dioxide dissolved in water. The partial charges on the hematite ions were estimated from *ab initio* calculations, with details outlined elsewhere [26]. See the Supporting Information for full list of force fields. The positions of hematite crystal were fixed; both water and CO_2 models used constraints to describe their covalent bonds, with the angle in CO_2 being flexible and fluctuating around 180 degrees. Time step was set to 0.5 femtoseconds. MDynaMix 5.1 molecular dynamics package by Lyubartsev and Laaksonen [27] with conventional velocity Verlet MD algorithm was employed to run the simulations in parallel on the Hexagon supercomputing facility at the University of Bergen. The systems were equilibrated for 1 million steps (0.5 ns), with the production run being 5+ million steps in duration.

Three characteristic features were observed when it came to behaviour of carbon dioxide in the model systems. The first and the more general observation was that carbon dioxide appeared to have a preference for being inside the 2 – 3 water layers which can be safely characterized as adsorbed phase (Figure 2a). On quite a few occasions illustrated in Figure 3, carbon dioxide molecules approached the hematite surface closely, taking positions among water adsorbed on the protruding irons. Two distinctive electrostatically-beneficent orientations were evident, one with one of the CO_2 oxygen atoms pointing directly at the oppositely-charged iron atom (Figure 2b), and a planar conformation where the carbon dioxide molecule orients itself to optimize all of its Coulomb interactions with both hematite ions (Figure 2c). This orientation will result in carbon dioxide lying flat against the surface. The third observation was that carbon dioxide showed signs of pronounced clustering as opposed to being dissolved in the water layer (see Figure 3). These observations should, however, be interpreted with amount of certain caution since only one specific number of carbon dioxide molecules and one specific temperature have been studied so far.

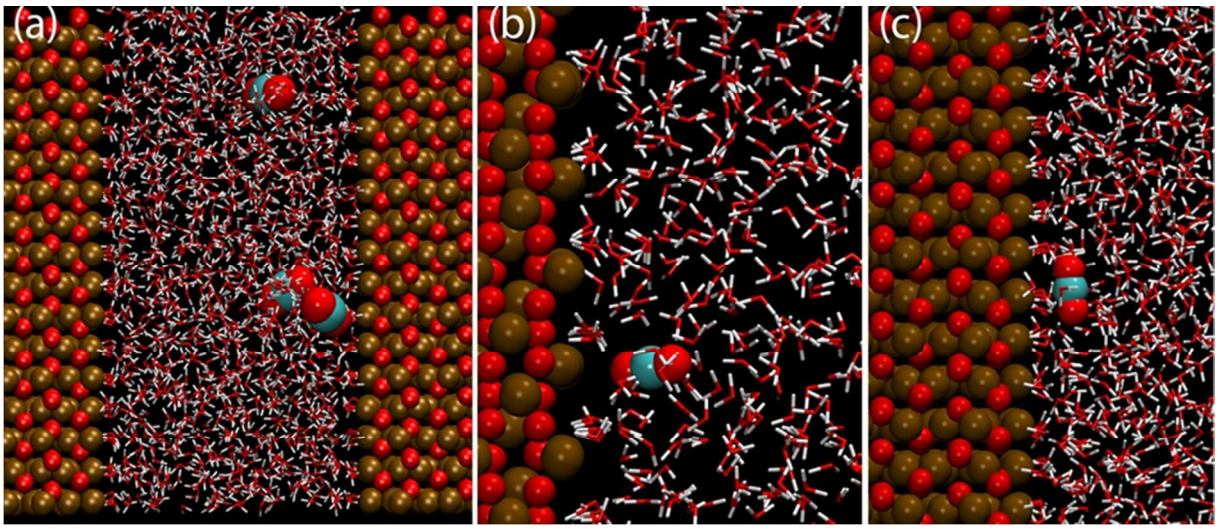

Figure 2 Characteristic behavior of carbon dioxide dissolved in water in the model water - CO2 - hematite system. (a) Preferred positioning and clustering (b) Normal orientation in coordination towards iron (c) Planar orientation. See text for details.

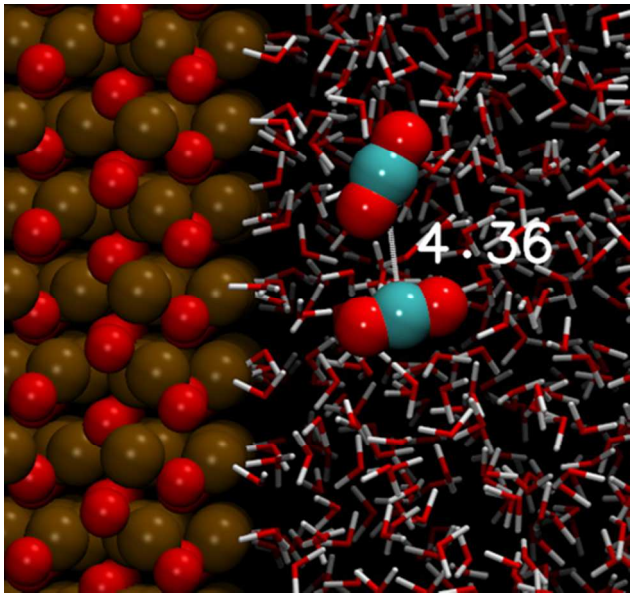

Figure 3: - Characteristic clustering of CO2 in proximity to hematite observed throughout the simulation run.

Findings yielded by visual inspections were further strengthened by quantitative analysis performed by means of pair correlation functions. Normalised RDFs calculated for carbon dioxide oxygen and all of the surrounding atoms exhibited two characteristic peaks – one that can be attributed to the carbon dioxide coordinating towards hematite and the other for carbon dioxide surrounded by water. Calculation of ideal-gas contributions to total chemical potential required the knowledge of carbon dioxide densities/partial molar volumes corresponding to these two states. The molar volumes were estimated following the first shell approximation of [16] (i.e. integrating the $4\pi r^2 g(r)$ curve until the first RDF minimum) and amounted to 936 and 861 kg/m^3, respectively, yielding the ideal-gas chemical potential of -31.86 kJ/mol and -32.05 kJ/mol. The residual chemical potential of adsorbed CO_2 was found to be -7.16 kJ/mol for 274 K, -7.88 for 278 K, and -7.36 kJ/mol for 283 K. The above values will correspond to the total chemical potential between -39.02 and -39.21 kJ/mol at 274 K. As discussed above, the adsorbed CO_2

molecules exhibited a complex dynamic adsorption behaviour that imposed substantial uncertainties in sampled averages, mainly due to electrostatic contributions. Within the present samplings, the uncertainties preclude a more rigorous interpretation than an interpolation based on the three temperature points (274 K, 278 K, 283 K):

$$\mu_{CO_2,ads}(T) = \left[-39.57 + 121.4\left(\frac{1}{T} - \frac{1}{274}\right)\right] \quad (7)$$

$$kJ/mole$$

The low chemical potential of water given by eq. (7) will prevent hydrate formation in water immediately affected by the hematite surface; it should be noted that water structure already approaches its bulk properties about 3 water layers away from hematite. Chemical potential estimated for carbon dioxide along the hydrate co-existence curve varied between -31.25 kJ/mol at 273.16 K to -30.07 kJ/mol at 284.74 K when using the Soave-Redlich-Kwong [28] equation for fugacity coefficients. Combined with equation (10) below for chemical potential of hydrate water, the values of adsorbed CO2 chemical potentials are too low to permit the carbon dioxide to form hydrate directly from adsorbed state and surrounding water.

In other words, the low chemical potential of adsorbed water will favour its drop-out via adsorption over liquid condensation, which will open two potential routes to hydrate formation. The first one will involve formation of hydrate from liquid water and adsorbed hydrate formers just outside the hematite surface. The estimated chemical potential for adsorbed CO_2 is substantially lower than that of carbon dioxide in hydrate along the co-existence curve. According to the first and the second laws of thermodynamics, no driving force will exist towards creation of hydrate from water and directly adsorbed carbon dioxide. The fact that CO_2 do show a preference for hematite will, however, also mean that it will be highly available at the interface between the adsorbed water film and the CO_2 stream, which would facilitate clustering and heterogeneous hydrate formation. When no other guests except for carbon dioxide are involved, the process of hydrate formation will be essentially identical to formation from liquid water in contact with carbon dioxide. Seafloor transport of carbon dioxide will normally entail conditions well inside the hydrate stability zone (temperature typically below 6 degrees Celsius and pressures above 50 bar). Since most current industrial strategies for hydrate risk evaluation involve the evaluation of water dew-point content, we will estimate the corresponding adsorption content, i.e. the water in carbon dioxide phase before dropping out as adsorbed phase on hematite.

Conventional hydrate risk assessment via water dew point versus analysis of water dropout as adsorbed phase

Figure 4 plots the ratio between the water mole fraction corresponding to the start of adsorption on hematite and the water dew point as a function of temperature for pressures ranging between 80 and 200 bars. As seen in this figure, the temperature dependency of the ratio is quite negligible, although the pressure dependency of the values themselves is quite significant (see fig. 5 illustrating the adsorption drop-out mole fraction of water as a function of pressure and temperature). As expected, there will be a slight increase in the adsorption preference with temperature. The thermodynamic properties for water phase and CO2 phase thermodynamics are described in [16, 17]. Figures 4 and 5 plot the water concentration in carbon dioxide obtained when equating the chemical potential of liquid and adsorbed water (equation (4) and (5), respectively). Our root-finding algorithm employed the bisection scheme, which converges fast

and is safer than the Newton-Raphson technique. Extending present risk analysis programs to include water adsorption on hematite will therefore be quite feasible.

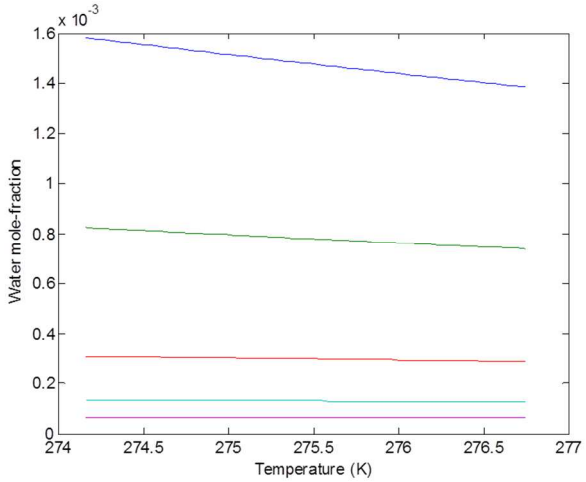

Figure 4: Estimated water dew-point concentrations in carbon dioxide solution. Curves are, from top to bottom, for pressures 110 bars, 120 bars, 135 bars, 150 bars and 200 bars.

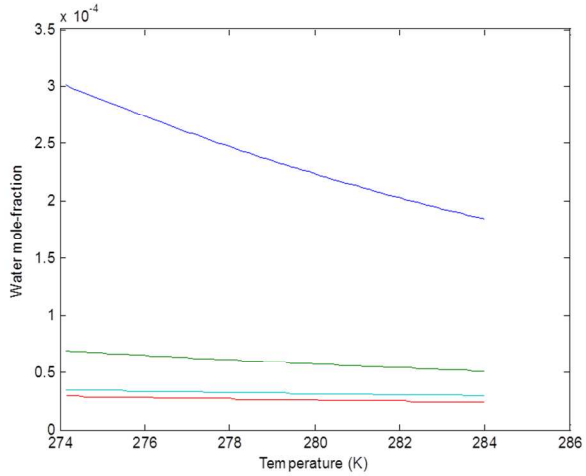

Figure 5 Limits of water mole-fraction in CO2 before drop-out as adsorbed on hematite. Upper curve is for 125 bars followed by 150 bars, 175 bars and 200 bars (bottom curve).

Thermodynamics of hydrate formation

Direct formation of hydrate from water dissolved in CO2 is thermodynamically feasible but highly unlikely compared to other options for water when in the order of 100 (based on estimated critical size for hydrate) water molecules needs to gather from a very dilute solution in CO2 and restructure into hydrate. There will also be a heat transport limitation since the surrounding CO2 fluid will work as a thermal insulator, making the dispersal of released heat to be rather problematic. Equations (4) and (5) will therefore represent the two most likely first steps to hydrate formation, while eqs. (8) and (9) below provide the minimum thermodynamic criteria for continued hydrate formation.

$$\mu_{w,hydrate}(T,P,\vec{x}_{hydrate}) \le \mu_{w,liquid}(T,P,\vec{x}_{liquid}) \quad (8)$$

$$\mu_{w,hydrate}(T,P,\vec{x}_{hydrate}) \le \mu_{w,adsorbed}(T,P,\vec{x}_{adsorbed}) \quad (9)$$

As indicated by findings of [10, 18], hydrate formation within the first adsorbed layer of water will be impossible due to extremely tight structure of water incompatible with the hydrate lattice. Furthermore, the average chemical potential of water for the first 4 water layers was found to be substantially lower than that of liquid water chemical potential. There might exist an opportunity for hydrate nucleation in the gap between the density peaks outside the hematite surface but this scenario needs a further investigation. In practice, this will mean that the process of hydrate formation from the adsorbed water will involve the liquid film 3 – 4 water diameters molecules away from the surface, with equation (8) being applicable as well. When polar and highly quadrupolar hydrate formers like H_2S and CO_2 are concerned, they will potentially add to the difference between the dew-point route to hydrate formation via equation (4) and adsorption route via equation (5) by adsorbing on hematite and providing a source of guest molecules.

We will apply the statistical mechanical model for water in hydrate that splits its chemical potential in two: the empty hydrate lattice and the impact of guest inclusion [1]:

$$\mu_{w,H} = \mu_{w,H}^{O} - \sum_{k=1,2} RTv_k \ln\left(1+\sum_i h_{ik}\right) \quad (10)$$

where H denotes hydrate phase, superscript 0 stands for empty hydrate lattice, v_k is the fraction of cavity of type k per water. For structure I hydrate, it will be equal to 1/23 for small cavities (20 water molecules) and 3/23 for large cavities (24 water molecules). h_{ik} is the canonical partition function for a cavity of type *k* containing a molecule of type *i*, given by the following equation:

$$h_{ik} = e^{\beta\left(\mu_i^H - \Delta g_{ik}^{inc}\right)} \quad (11)$$

where β is the inverse of the gas constant times temperature and Δg_{jk}^{inc} is normally referred to as the free energy of inclusion; it describes the effect that the inclusion of "guest" molecule *i* will have on hydrate water lattice [1]. At equilibrium, chemical potential μ_i^H of guest *i* has to be the same as in the phase where it was extracted from. The hydrate content of all gas components can be estimated using their ideal-gas chemical potentials corrected for ideal gas mixing and fugacity coefficients [16, 17] pertaining to these components in carbon dioxide. The chemical potential of liquid water will be slightly affected by presence of dissolved hydrogen sulfide and carbon dioxide, with particularly the content of hydrogen sulfide in the different phases impacting the results significantly. Solving eq. (4) under given temperature and pressure will yield the highest possible water content in CO2 before it starts dropping out. In contrast to that, the hydrate formation solution will only have one degree of freedom rather than two. This means that hydrate-formation pressure will have to be determined in an iterative loop together with equations (4), (8) and (10) to ensure that gas composition and chemical potential, as well as liquid water composition and chemical potential will be consistent with the actual hydrate forming pressure that satisfies the following equation:

$$\mu_w^{O,H} - \sum_{k=1,2} RTv_k \ln\left(1+\sum_i h_{ik}\right) = \mu_{i,\text{liquid}}^{purewater}(T,P) + RT\ln\left[x_{i,\text{liquid}}\gamma_{i,\text{liquid}}(T,P,\vec{x}_{liquid})\right] \quad (12)$$

where subscript *i* denotes component in liquid water phase. $\gamma_{i,\text{liquid}}$ is the activity coefficient of component *i* in the liquid water phase.

Note that the chemical potentials for empty hydrate estimated from Kvamme & Tanaka [1] have been proven to have predictive capabilities, which makes empirical formulations redundant. If the estimated hydrate formation pressure is lower than the local pressure, hydrate will form via this particular route.

Besides being unable to reach equilibrium, as discussed in the introduction, the system under consideration will be characterized by drastic differences in hydrate-forming abilities of impurities dissolved in CO_2. H_2S is an extremely aggressive hydrate former, while nitrogen is the absolute opposite. So a more realistic evaluation of this possible route to hydrate formation needs to start from a dew-point calculation for water with H_2S and CO_2 as the condensing components together with water – similar to the approximations above. If the dew-point pressure is lower than the local pressure, water will drop out as a liquid; one can therefore assume the availability of free water and subsequent formation of hydrate with the lowest free energy. In contrast to the "classical" calculations that assume the conventional hydrate formation from "bulk" gas, our approach involves an analysis of the absolute lowest free energy hydrate that could be formed from a given carbon dioxide mixture, i.e. minimizing Gibbs free energy below with respect to hydrate formation pressure, noting that the system cannot reach equilibrium.

$$G^H = \sum_i x_i^H \mu_i^H \quad (13)$$

The non-equilibrium hydrate description due to Kvamme et. al. [2] can then be applied to follow the gradients in free energies until the carbon dioxide phase is depleted of the most "aggressive" hydrate former (hydrogen sulfide). The utilization of equation (13) will require knowledge of hydrate composition; it can be found from the statistical mechanics involved in the adsorption model for hydrate, equations (10) and (11), and can be written in the following form:

$$\theta_{ik} = \frac{x_{ik}^H}{v_k\left(1-x_T\right)} = \frac{h_{ik}}{1+\sum_i h_{ik}} \quad (14)$$

where θ_{ik} is the filling fraction of component *i* in cavity type *k*, x_{ik}^H is the mole fraction of component *i* in cavity type k, x_T is the total mole fraction of all guests in the hydrate and v_k is, as defined above, the fraction of cavities per water of type *k*.

The free energy of inclusion Δg_{jk}^{inc} appearing in equation (11) can be estimated following Kvamme & Tanaka [1]. At this stage, no attempts have been made to tune the model empirically to fit experimental data available in open literature. Thermodynamic consistency has been a high priority throughout this work. Since the molecular interaction model for CO_2 in this work is different from that of Kvamme & Tanaka [1], new free energy of inclusion functions parameters for this model, as well as for the H_2S model, have been estimated and listed in table 1 below (complementary to table 5 of Kvamme & Tanaka [1]). Though there is evidence that CO_2 can enter small cavities, we have chosen to ignore this factor, since its stabilization impact is questionable, and it is quite uncertain whether CO_2 is able to fill the small

cavities under dynamic conditions. So at least within the scope of this, study we will assume that CO_2 can only enter the large cavities. The free energies of CO2 inclusion can be found in Kvamme et.al. [18, 19].

Table 1. Parameters used to calculate the free energy of inclusion into structure I as an expansion series

$$\Delta g^{inclusion} = \sum_{i=0}^{5} k_0 \left[\frac{T_C}{T} \right]^i$$

for small and large cavity fillings of H2S. T_C is critical temperature of pure H_2S.

Parameter	Small cavity	Large cavity
k_0	-97.990401	-97.965227
k_1	111.553880	138.932970
k_2	-60.758909	-41.731057
k_3	-31.817796	-20.754364
k_4	-14.963883	-19.723404
k_5	26.370947	13.831618

Hydrogen sulfide, a well-known and extremely vigorous hydrate-former was considered to be one of the impurities likely to significantly impact the process of hydrate formation during pipeline transport. Due to low chemical potential of water at the hematite surface, hydrate formation will only be possible outside the first 3 – 4 adsorbed layers. Out all of the considered impurities, CO_2 and H_2S will dominate hydrate formation. Since CO_2 will constitute the main fluid phase, and CO_2 dissolved in water will have a lower chemical potential when dissolved in water than the fluid CO_2, the latter will be the most likely CO_2 source for hydrate formation. As an example, Figure 6 presents the solubility of H_2S in water corresponding to its initial mole fraction of 0.0001 in the CO_2 phase. The fugacity coefficients of H_2S and CO_2 have been estimated using the SRK [28] equation of state. The same equation has been applied to calculate the partial molar volumes of H_2S required for calculation of estimate the ideal gas chemical potential. The moments of inertia were those of the H_2S model due to Kristóf and Liszi [29] used in molecular dynamics studies described later.

Figure 7 presents chemical potential of water in a liquid state and a hydrate lattice as a function of stabilisation at 100 bar. Since these chemical potentials are plotted for comparison purposes only, the quite negligible Pointing correction have been omitted for all curves. The chemical potential of liquid water and empty-clathrate water was calculated following Kvamme & Tanaka [1]. Hydrate stabilisation by means of dissolved H_2S only (the upper dashed curve) means that it is only the chemical potential of H_2S in water solution that enters equation (9) through the cavity partition function of equation (10). The lower dashed curve combines the contribution to the cavity partition function from the fluid CO_2, as well as additional stabilisation from the cavity partition function for small and large cavities due to dissolved H_2S. Similar to hydrate formation from the fluid phase, water-dissolved H_2S can only contribute to stabilization of a CO_2-dominated hydrate rather than form a hydrate of its own.

Similar calculations performed for H_2S mole fraction of 0.001 in CO_2 and pressure of 100 bar yielded the solubility of H_2S plotted in figure 8 and resulting water chemical potentials plotted in fig. 9. Results corresponding to the H_2S mole fraction of 0.005 are plotted in figures 10 to 12.

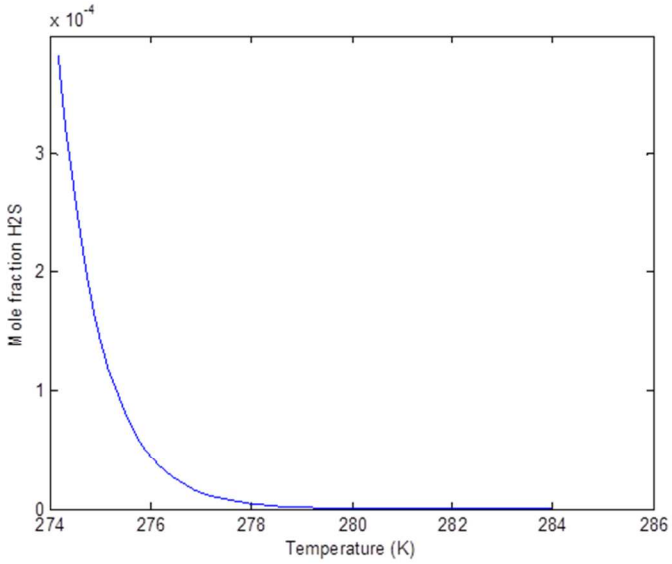

Figure 6. Estimated solubility of H2S in the water phase in case of H2S mole fraction in CO2 equal to 0.0001 at 100 bar pressure.

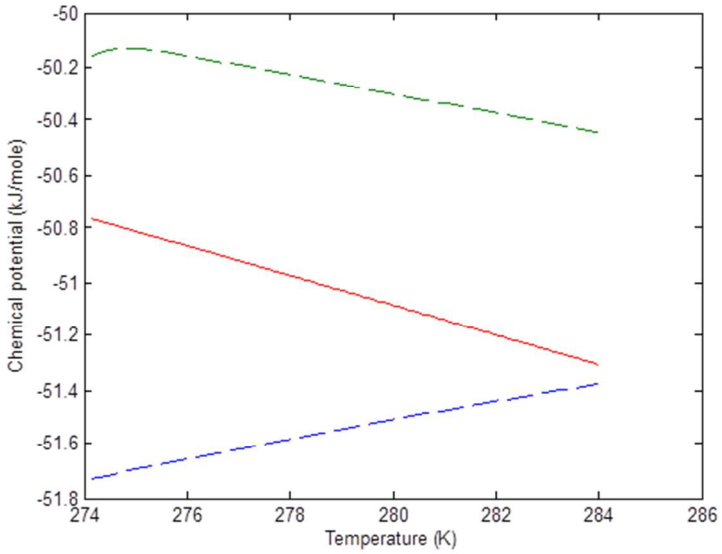

Figure 7 Chemical potential of water as liquid (solid) and in hydrate stabilised by dissolved H2S only (upper dashed curve) and H2S dissolved in water and CO2 from the fluid phase (lower dashed curve). Pressure equal to 100 bar and H2S mole fraction in CO2 is 0.0001.

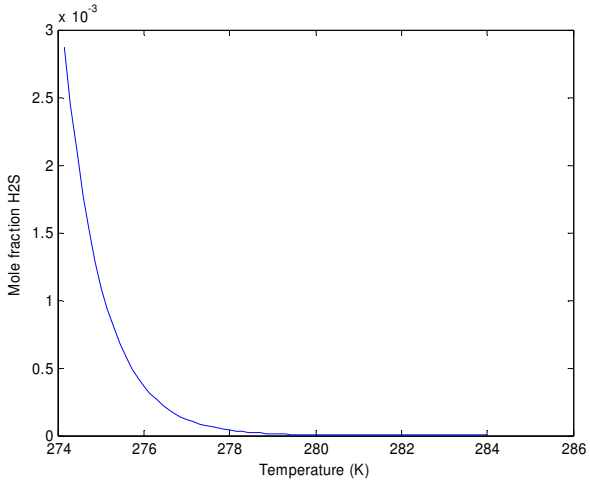

Figure 8. Estimated solubility of H2S in the water phase for H2S mole fraction in CO2 equal to 0.001.

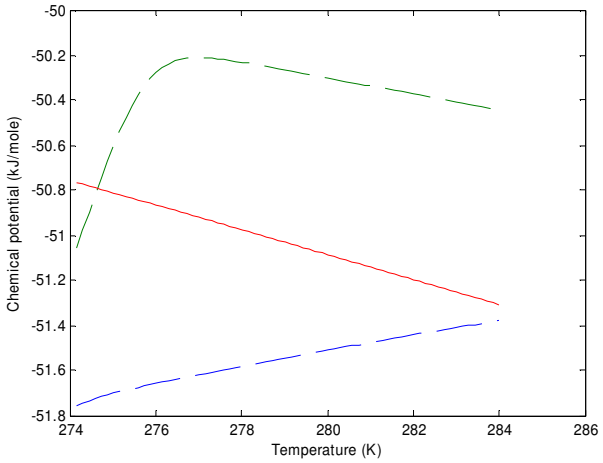

Figure 9. Chemical potential of water as liquid (solid) and in hydrate stabilised by dissolved H2S only (upper dashed curve) and H2S dissolved in water and CO2 from the fluid phase (lower dashed curve). Pressure equal to 100 bar and H_2S mole fraction in CO_2 is 0.001.

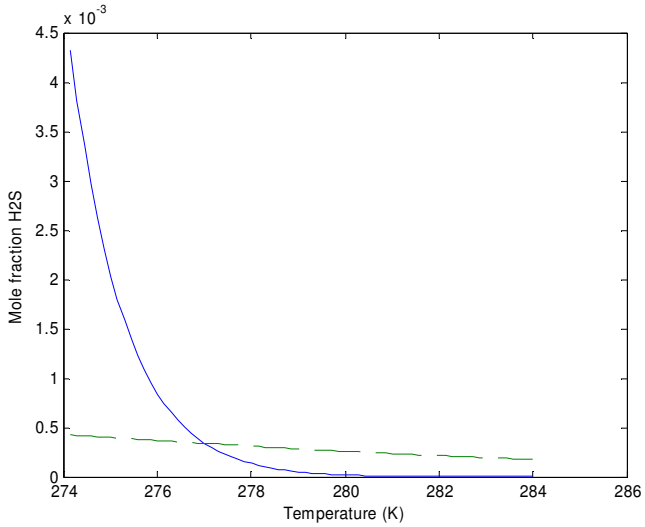

Figure 10. Estimated solubility of H_2S in the water phase in case of H_2S mole fraction in CO_2 equal to 0.005 and pressures of 100 bar (solid) and 200 bar (dashed).

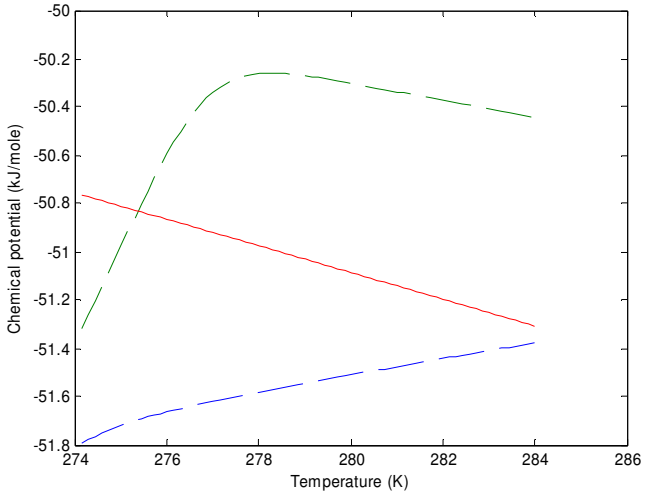

Figure 11. Chemical potential of water as liquid (solid) and in hydrate stabilised by dissolved H2S only (upper dashed curve) and H2S dissolved in water and CO2 from the fluid phase (lower dashed curve). Pressure equal to 100 bar and H_2S mole fraction in CO_2 is 0.005.

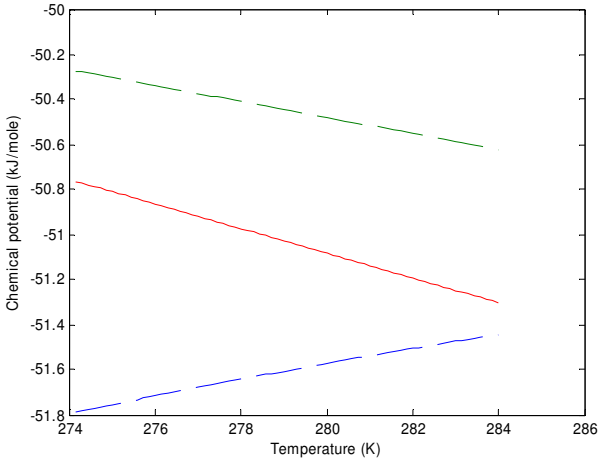

Figure 12. Chemical potential of water as liquid (solid) and in hydrate stabilised by dissolved H2S only (upper dashed curve) and H2S dissolved in water and CO2 from the fluid phase (lower dashed curve). Pressure equal to 200 bar and H_2S mole-fraction in CO_2 0.005.

In the pressure range between 100 and 200 bars, hydrogen sulfide shows a preference for the CO_2 phase that increases with pressure. When analysed in their entirety, the above results point to an important conclusion: when hydrogen sulphide concentration in CO_2 is high at lower pressures (mol fraction of 0.005 used as an example), H_2S becomes capable of forming a separate aqueous-phase hydrate. In addition, it will assist in stabilisation of CO_2-dominated hydrate. This means that both nucleation and hydrate formation from the adsorbed phase can be expected to be very fast under these conditions.

Molecular dynamics modelling of hematite-water-H_2S system

Given that the hydrogen sulfide molecule bears a significant resemblance to that of water, we believed it was important to investigate their relative affinities towards rust surfaces by means of atomistic simulations. An interfacial model system was constructed (Figure 13), virtually identical to the ones described above, with the only difference being in carbon dioxide replaced by a flexible hydrogen sulfide model of Kristóf and Liszi [29]. This model is a 4-site planar model that, unlike TIP4P water model, has 4 partial charges, with sulfur represented by two oppositely charged sites. While the positively charged site also carries the van der Waals interaction, the negatively charged massless site is shifted alongside the bisector of the H-S-H towards the hydrogens. Since Shake-type algorithms are known to struggle with constraints like these, the H2S was modeled as fully-flexible molecule with five bonds, four angles and one improper dihedral used to maintain the planar geometry in the presence of strong interactions between H_2S and hematite. Since this model is Lennard-Jones in form, CLAYFF [30] force field parameters were employed to estimate interatomic interaction between H2S and hematite via conventional Lorentz-Berthelot rules (see Supporting Information).

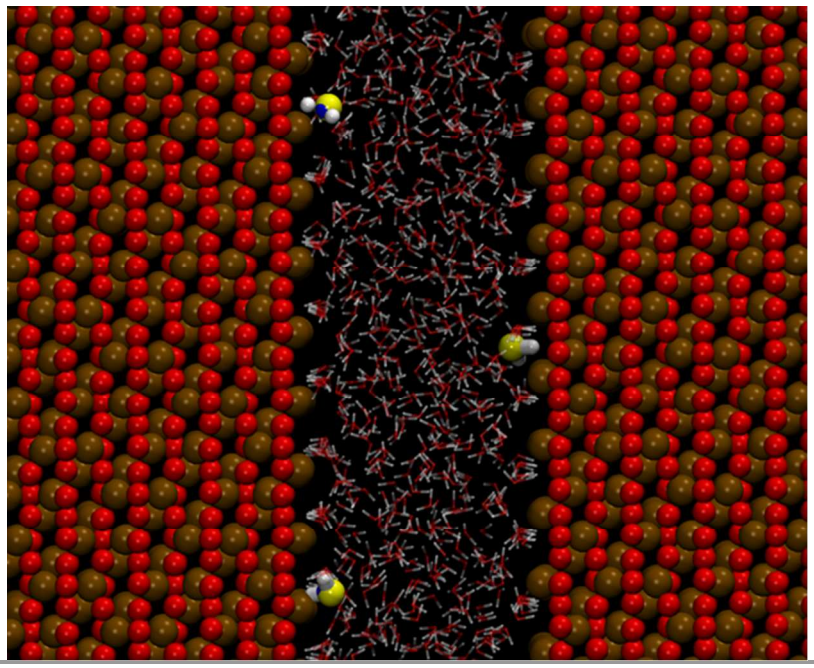

Figure 13. A representative snapshot from model water – H_2S – hematite system. Note the preferred positioning of hydrogen sulfide.

The hydrogen sulfide behaviour has shown itself to be much more similar to water than carbon dioxide when it came to interactions with hematite. All three H_2S molecules have quickly found their way to the surface and attached themselves to it. As seen in Figure 13, hydrogen sulfide showed a strong affinity for specific surface sites, with the H_2S hydrogen coordinated towards the oxygen ions in hematite. The comparison of pair correlation functions in Figures 14 and 15 shows that hydrogen sulfide and water were positioned at about the same distance from both iron and oxygen hematite sites, with the first peak in hydrogen – oxygen RDF located at 2.18 Å (Figure 14). The RDF plotted in Figure 15 indicates that the hydrogen atom was located further away from hematite iron than hematite oxygen (3.08 Å vs 2.17 Å), with the first peak of the H_2S-hydrogen RDF possessing a distinct shoulder absent in the water-hydrogen RDF.

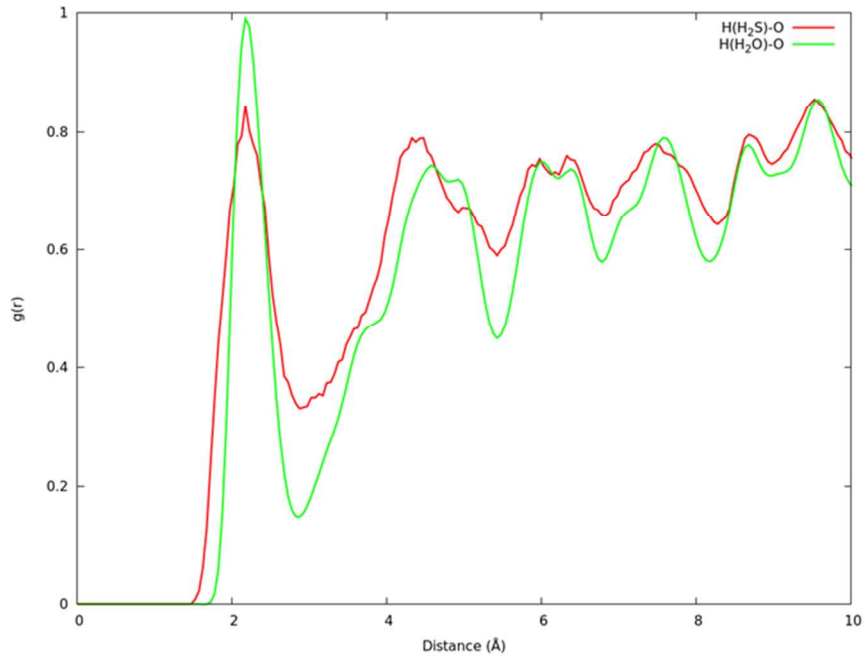

Figure 14. Pair correlation functions for oxygen in hematite and hydrogen in hydrogen sulfide (green) and water (red).

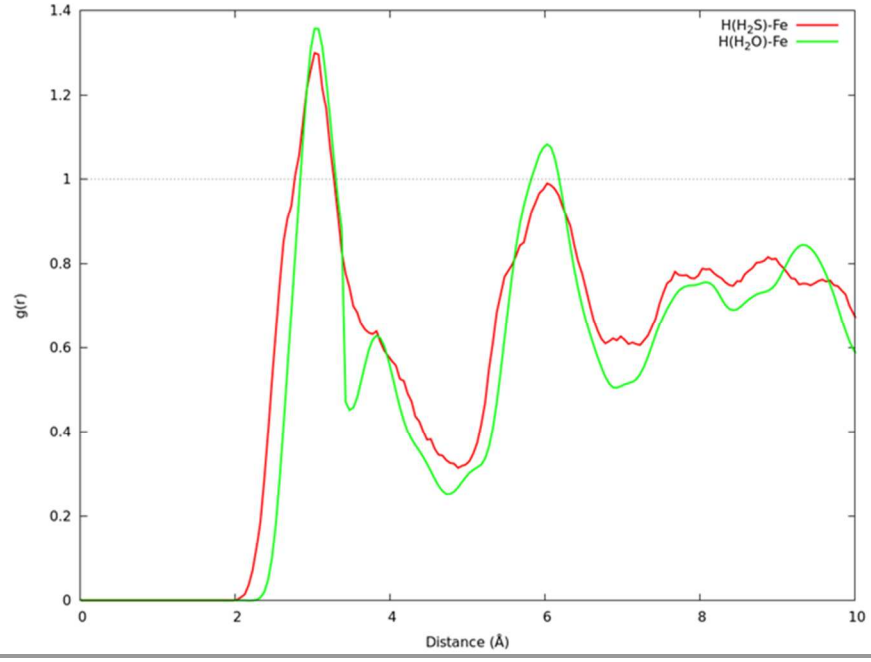

Figure 15. Pair correlation functions for iron in hematite and hydrogen in hydrogen sulfide (green) and water (red).

None of the adsorbed hydrogen sulfide molecules left the hematite surface during the 6+ nanosecond-long simulation. This behaviour was in strong contrast to that of water whose first adsorbed layer was completely replaced within 35 picoseconds. This indicates that hydrogen sulfide is more tightly bound to the rust surface than water. The affinity of hydrogen sulfide for

the rust surface was not entirely unexpected, given the geometry and the distribution of partial charges in the model in question. The dipole moment of Kristóf and Liszi H_2S is 1.4 D compared to experimentally estimated value of 1.0 D [29]. The H2S preferences were confirmed further by comparison of potential energy values.

We have used the technique of thermodynamic integration via a polynomial route due to Mezei [31] to estimate the residual chemical potential of adsorbed H_2S at 274.15K. The integration yielded -11.0 +/- 4.0 kJ/mol. Similarly, -10.0 +/- 3.0 kJ/mol and -10.0 +/- 3.0 kJ/mol were obtained at 278.15K and 283.15K, respectively. It should be cautioned that H_2S seemed to be undergoing a phase transition during a certain portion of its polynomial path route, which if included, would lead to chemical potential lower than the values listed here. Combining the residual chemical potentials and the ideal contributions made it evident that H_2S exhibited a much higher preference for the hematite surface than carbon dioxide. Partial molar volumes estimated for adsorbed H_2S using the integration of *g(r)* between hematite iron and H_2S sulfur produced the ideal-gas chemical potential of -35.4 kJ/mol, compared to ideal-gas chemical potential of -34.4 kJ/mol for H_2S dissolved in water. Given the specific adsorption pattern, an average of these two values has been considered a good enough approximation, bringing the total chemical potential of adsorbed H_2S to -45.8 kJ/mol at 274 K. The total chemical potentials at 278.15K and 283.15K will amount to -45.2 and -45.3 kJ/mol, respectively. Thus the total chemical potential of adsorbed H_2S will be lower than that of CO_2 by about 6 kJ/mol. The inclusion of the aforementioned phase transition may skew this further in favour of the H_2S.

Chemical potential of water when in hydrate formed from adsorbed H_2S and in bulk water is plotted in figure 16. Adsorbed CO_2 will be unable to stabilize the hydrate on its own and only provide minor additional stabilization for hydrate formed from water and adsorbed H_2S.

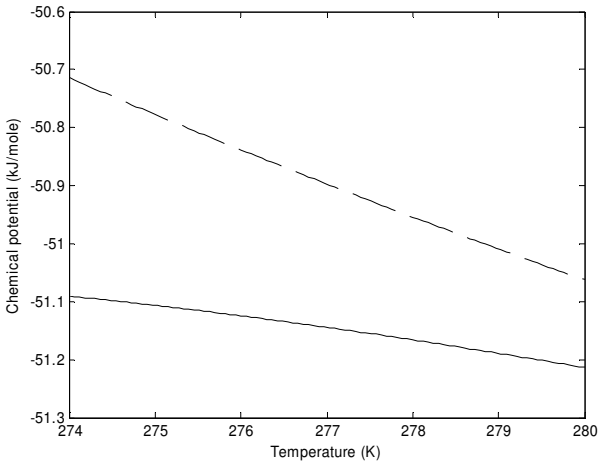

Figure 16. Chemical potential for water in hydrate (solid) as stabilized from adsorbed H_2S at 100 bar and liquid water chemical potential (dashed) under same conditions.

The use of Lorentz-Berthelot mixing rules (eq. (2)) with k_{ij} set to zero for cross interactions between H_2S and hematite offers a typical example of unrealistically strong adsorption of H_2S to the surface. Introduction of positive k_{ij} with values ranging between zero and one for these interactions will reduce the short-range attraction contribution to the adsorption between H_2S and hematite. It may be advisable to conduct a detailed study on the way the varying the k_{ij} will affect

the adsorption characteristics. Decreasing the "effective" cross interaction energies through equation (2) will lead to weaker adsorption energies. Although this effect can also expected to involve an entropy increase for the adsorbed H_2S, the net effect would raise the total adsorbed chemical potential. Within the limited scope of this work, we illustrate potential effects of limited increases in H_2S adsorbed potential on hydrate formation from liquid water and adsorbed H_2S in figure 17.

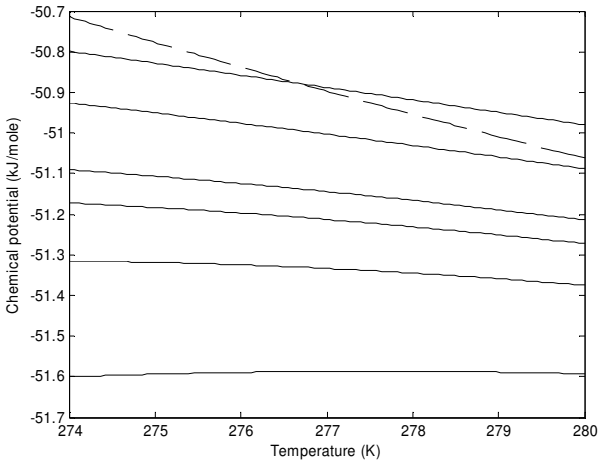

Figure 17. Chemical potential for water in hydrate (solid) as stabilized from adsorbed H_2S at 100 bar and estimated adsorbed chemical potential (including ideal gas contribution) by factors of 0.90, 0.95, 0.98, 1.0, 1.05 and 1.10 from top to bottom. Liquid water chemical potential under the same conditions is plotted as dashed curve.

Figure 17 reflects the fact that H_2S is an extraordinary good hydrate former due to its favourable dipole moment, which is also indicated by its free energy of inclusion (equation (11) and table 1). Even if the adsorption chemical potential were lower than the values predicted by the H_2S model of Kristóf and Liszi [29], our estimates plotted in figure 17 suggest that H2S molecules may still be captured by hydrate. Both CO_2 and H_2S will follow water condensing onto hematite. Realistic adsorption and corresponding chemical potentials would, however, require development of improved new models for H_2S and CO_2, unless a correction could be applied to the mixing rules in equation (2) to account for the transition from a fluid phase to an adsorbed state. These considerations are outside the scope of this study and require a separate investigation.

The use of SPC/E rather than TIP4P water model in the adsorption calculations for CO_2 and H_2S imposes an unknown bias, although we expect this bias to be small based on the similarities in the solvation properties of SPC/E and TIP4P in. As such, there are also some model differences in the adsorption studies in which SPC/E was applied. There might be minor differences between TIP4P and SPC/E in structuring around the adsorbed H_2S and CO_2 and also slight differences due to differences in entropy generation caused by differences in thermostats. But none of these effects are expected to have substantial impact on the sampled results. We should also keep in mind that adsorbed water chemical potentials are based on the quantum chemistry techniques and not entirely unique since different approximations may result in different partial charge distributions on the hematite surface. The values used in the analysis here were the second set from figure 2 in Kvamme et.al. [10]. Hematite is only one of the several rust forms but it is thermodynamically the most stable one and expected to dominate. Reactions with carbon dioxide might to some degree convert hematite into iron carbonate and in follow up studies it might be worthwhile to investigate possible rust forms

that can result from the carbon dioxide reactions.

Another advantage of the chemical potentials made available through this study is the opportunity they provide for studying complex phase transition scenarios using advanced concepts like density functional theory or phase field theory. But even simpler kinetic theories like the classical theory or the Multicomponent Diffuse Interface Theory (MDIT) theory [7, 8] will be able to incorporate these data and thus provide kinetic models with a stronger theoretical basis than the commonly applied model due to Kim et.al. [32]. Note that the MDIT reduces to the classical theory in the limit of zero interface thickness. Even simpler schemes can be added to existing industrial platforms for hydrate risk evaluation by simply adding the different additional routes to hydrate formation and estimate the conditions for which these events are likely to happen.

In addition to water and hydrogen sulfide, the carbon dioxide streams will most like contain methane, argon and nitrogen. These components are non-polar, with very low water solubility and thus virtually no chance to compete with water for hematite adsorption. Thus, the only potential effect of these components would be to provide additional stabilisation of carbon dioxide-dominated hydrate; this effect would be trivial to evaluate by any hydrate equilibrium code (route 6 in Figure 1).

A challenge with evaluating adsorbed chemical potentials is the lack of experimental data for water, hydrogen sulfide and carbon dioxide adsorbing simultaneously on hematite. Even if one adjusts the mixing rule following equation (2), no experimental to validate a given parameter set is available at present. Pure *ab initio* calculations are limited in size and even if there are options for adding imitated water fields, it is still unverified how well this can represent this very inhomogeneous adsorbed system. The best option would include implementing a Car-Parrinello method [33] to investigate varying mole fractions of hydrogen sulfide adsorbed so as to subsequently regress the sampled *ab initio* based fluid/mineral interactions to the k_{ij} factors (equation 3). With similar procedure applied for carbon dioxide adsorption and adsorption of water, hydrogen sulfide, and carbon dioxide mixture, the goal would be to find adsorbed chemical potential as function of temperature, pressure and adsorbed concentration. These chemical potentials can then be utilized in combined mass-balance and quasi-equilibrium calculations for adsorbed mole fractions. More specifically, this approach would involve solving the quasi-equilibrium criteria as given by equation (5) but now applied simultaneously for hydrogen sulfide and carbon dioxide in addition to water. This would in effect be a type of flash calculation for adsorbed/gas.

Conclusions

Pipeline transport of dense carbon dioxide containing various impurities will entail several risk factors related to water that accompanies CO2. In addition to water, carbon dioxide stream originated from natural hydrocarbon systems will typically contain methane and hydrogen sulfide. Solid water-wet surfaces, like rust, may promote hydrate formation because they may be more advantageous for water to condense on than drop out in the form of liquid water. In this work, we have investigated the impact of solid surfaces on water drop-out in its bulk solution in carbon dioxide versus drop-out in the form of adsorbed water and its consequences for hydrate formation. We have shown that while liquid water would be thermodynamically favoured to adsorb on hematite (one of dominant rust forms), its lower chemical potential of in the immediate adsorbed layer will make it unlikely that hydrate will form inside the 3 – 4 layers of water closest to the hematite surface. In addition to providing a preferred surface for water drop-out, the presence hematite will promote a vigorous adsorption of polar hydrate formers like hydrogen sulfide. This may create very favourable conditions for heterogeneous hydrate formation. Force field derived from the liquid state studies may not be appropriate for the adsorbed state since the characteristic frequencies of motion (translation and rotation) of adsorbed molecules will be entirely different, which will significantly affect their corresponding impact. Specifically, we have demonstrated that a widely-used model of hydrogen

sulphide that successfully reproduces vapour-liquid equilibria will result in very unrealistic adsorption.

To ensure a consistent treatment of chains of indirect interactions, it is argued that rather than assigning entirely independent fitted cross terms between liquid-phase molecules and the mineral surfaces, it would be preferable to investigate a possible adjustment of classical Lorentz-Berthelot mixing rules.

Hydrogen sulfide is an extremely vigorous hydrate-former; estimates presented in this work suggest that even unrealistically strong adsorption might still fail to prevent it from forming a mixed hydrate. The hematite adsorption of carbon dioxide will be of less significance but there is still need for more fundamental studies of carbon dioxide-hematite interactions which could make use of efficient algorithms that couple *ab initio* calculations for direct solid surface -- fluid interactions with surrounding interactions based on classical molecular dynamics.

Acknowledgements

We gratefully acknowledge the grant and support from the Research Council of Norway through the following projects: SSC-Ramore, "Subsurface storage of CO_2 - Risk assessment, monitoring and remediation", Research Council of Norway, project number: 178008/I30, FME-SUCCESS, Research Council of Norway, project number: 804831, PETROMAKS, "CO_2 injection for extra production", Research Council of Norway, project number: 801445. Funding from Research Council of Norway, TOTAL and Gassco through the project "CO_2/H_2O+" is highly appreciated.

Notes and references

[a] Universitetet i Bergen, Institutt for Fysikk og Teknologi, Allégaten 55, N-5007 Bergen, Norge. Fax: +47 55589440; Tel: +47 55583310; E-mail: bjorn.kvamme@ift.uib.no.

Electronic Supplementary Information (ESI) available: [Supporting Information detailing force fields used in molecular dynamics simulations]. See DOI: 10.1039/b000000x/

[1] B. Kvamme, and H. Tanaka, "Thermodynamic Stability of Hydrates for Ethane, Ethylene, and Carbon Dioxide", *J. Phys.Chem.*, 1995, **99**, 7114-7119.

[2] B. Kvamme , T**.** Kuznetsova , P.-H**.** Kivelæ and J**.** Bauman, **"**Can hydrate form in carbon dioxide from dissolved water?**",** *Phys. Chem. Chem. Phys.*, 2013, Advance Article DOI: 10.1039/C2CP43061D

[3] B. Kvamme, O.K. Førrisdahl, *"Polar guest-molecules in natural gas hydrates."* Fluid Phase Equilibria, 83, 1993, 427.

[4] Kvamme, B., "Kinetics of sour gas solubility in water and the role of selective adsorption onto liquid water", 1999, unpublished (contractor imposed confidentiality).

[5] Bjørn Kvamme, *"Feasibility of simultaneous CO2 storage and CH4 production from natural gas hydrate using mixtures of CO2 and N2"*, 2014, Canadian Journal of Chemistry, in press.

[6] Bjørn Kvamme, *"Injection of CO2/N2 mixtures into CH4 hydrate – will it provide safe long terms storage of CO2?"*, 2015, AAPG Interpretation, submitted.

[7] B. Kvamme, "Kinetics of Hydrate Formation from Nucleation Theory", *Int. J. Offshore Polar Eng.*, 2002, **12**(4), 256-263.

[8] B. Kvamme, "Droplets of Dry Ice and Cold Liquid CO_2 for Self-Transport of CO_2 to Large Depths", *Int. J. Offshore Polar Eng.*, 2003, **13**(2), 139-146

[9] B. Kvamme, A. Graue, E. Aspenes, T. Kuznetsova, L. Gránásy, G. Tóth, T. Pusztai, G. Tegze, "Kinetics of solid hydrate formation by carbon dioxide: Phase field theory of hydrate nucleation and magnetic resonance imaging" *Phys. Chem. Chem. Phys.*, 2004, **6,** 2327-2334.

[10] B. Kvamme, T. Kuznetsova and P.-H. Kivelæ, "Adsorption of water and carbon dioxide on hematite and consequences for possible hydrate formation" *Phys. Chem. Chem. Phys.,* 2012, **14**, 4410-4424.
[11] L. J. Noake, D. L. Katz, "Gas Hydrates Of Hydrogen Sulfide-Methane Mixtures", Petroleum Transactions, AIME SPE 367-0, 135-137.
[12] J. P. Schroeter, R. Kobayashi, M. A. Hildebrand, "Hydrate Decomposition Conditions in the System H2S-Methane-Propane", *Ind. Eng. Chem. Fundam.*, 1983, **22***,* 361-364.
[13] H. J. C. Berendsen, J. R. Grigera, T. P. Straatsma. "The missing term in efective pair potentials", *J. Physs. Chem.*, 1987, **91**, 6269-6271.
[14] W. L. Jorgensen and J. D. Madura, Temperature and size dependence for Monte Carlo simulations of TIP4P water, *Mol. Phys.*, 1985, **56,** 1381-1392.
[15] M. Levitt, M. Hirshberg, R. Sharon, K. E. Laidig, V. Daggett. "Calibration and Testing of a Water Model for Simulation of the Molecular Dynamics of Proteins and Nucleic Acids in Solution", *J. Phys. Chem. B*, 1997, 101**,** 5051-5061.
[16] D. Chandler. "Equilibrium theory of polyatomic fluids", in *Studies in Statistical Mechanics* **8**, 275-340 (J.L. Lebowitz and E.W. Montroll, eds.), North Holland, Amsterdam (1982).
[17] B.M. Ladanyi, D. Chandler. "New type of cluster theory for molecular fluids: Interaction site cluster expansion", *J. Chem. Phys*., 1975, **62**, 4308-4324.
[18] B. Kvamme, T. Kuznetsova, B. Jensen, S. Stensholt, J. Bauman, S. Sjøblom, K. N. Lervik, "Investigating chemical potential of water and H2S dissolved into CO2 using molecular dynamics simulations and Gibbs-Duhem relation", 2014, submitted to Fluid Phase Equilibria.
[19] Bjørn Kvamme, Tatiana Kuznetsova, Bjørnar Jensen, Sigvat Stensholt, Jordan Bauman, Sara Sjøblom and Kim Nes Lervik, "Consequences of CO2 solubility for hydrate formation from carbon dioxide containing water and other impurities, *Phys. Chem. Chem. Phys.*, 2014, 16 (18), 8623 – 8638
[20] Bjørn Kvamme, Tatiana Kuznetsova, and Martin Haynes, "*Molecular dynamics studies of water deposition on hematite surfaces*", 2012, AIP Conf. Proc. 1504, 780-783, DOI: 10.1063/1.4771809
[21] Bjørn Kvamme, Tatiana Kuznetsova, Pilvi-Helina Kivelæ and Jordan Bauman, "Can hydrate form in carbon dioxide from dissolved water?", 2013, PCCP, 15 (6), 2063 - 2074.
[22] W. L. Jorgensen, J. D. Madura, C. L. Swenson, «Optimized intermolecular potential functions for liquid hydrocarbons", *J. Am. Chem. Soc.*, 1984, ***106***, 6638–6646.
[23] N. H. de Leeuw, T. G. Cooper, "Surface simulation studies of the hydration of white rust Fe(OH)(2), goethite alpha-FeO(OH) and hematite alpha-Fe2O3." *Geochimica et Cosmochimica Acta*, 2007, **71**(7), 1655-1673.
[24] S. Tsuzuki, T. Uchimaru, K. Tanabe, S. Kuwajima, N. Tajima, T. Hirano. "Refinement of nonbonding interaction parameters for carbon dioxide on the basis of the pair potentials obtained by MP2/6-311+G(2df)-level ab initio molecular orbital calculations." *J. Phys. Chem.*, 1996, **100**(11), 4400-4407.
[25] M. In Het Panhuis, C. H. Patterson, R. M. Lynden-Bell, "A molecular dynamics study of carbon dioxide in water: diffusion, structure and thermodynamics", *Mol. Phys*, 1998, **94**, 963-972.
[26] J. T. Vassdal (2010). "Molekylærdynamiske studier av vannadsorpsjon på hematitt." Institutt for fysikk og teknologi. Master thesis, University of Bergen, June 2010.
[27] A. P. Lyubartsev, A. Laaksonen. "MDynamix - A scalable portable parallel MD simulation package for arbitrary molecular mixtures." *Comput. Phys. Commun*. 2000, **128**, 565-589.
[28] G. Soave, "*Equilibrium constants from a modified Redlich-Kwong equation of state", Chem. Eng. Sci.*, 1971, **27**, 1197-1203.
[29] T. Kristóf, J. Liszi, "Effective Intermolecular potential for Fluid Hydrogen Sulfide", *J. Phys. Chem.,* 1997, **101**, 5480-5483.

[30] R. T. Cygan, J.-J. Liang, A. G. Kalinichev, "Molecular Models of Hydroxide, Oxyhydroxide, and Clay Phases and the Development of a General Force Field", *J. Phys. Chem. B*, 2004, **108**, 1255–1266.
[31] M. Mezei, "Polynomial path for the calculation of liquid state free energies from computer simulations tested on liquid water", *J. Comput. Chem.,* 1992*,* **13***,* 651-656.
[32] H. Kim, P. Bishnoi, R. Heidemann, S. Rizvi. "Kinetics of methane hydrate decomposition", *Chem. Eng. Sci.*, 1987, **42**, 1645-1653.
[33] R. Car, M. Parrinello. "Unified Approach for Molecular Dynamics and Density-Functional Theory", *Phys. Rev. Lett.,* **55,** 1985, 2471–2474.

